Chapter 6

On the evolution of magnetic shock wave in the mixture of gas and small solid dust particles

"Go down deep enough into anything and you will find mathematics."

-Dean Schlicter

6.1 Introduction

The study of effect of small solid dust particles on the evolution of weak shock wave has gained significance due to its application in the area of medical sciences and engineering e.g., in treatment of cancer, kidney stone disease, orthopedics etc. The weak shock waves are utilized to break the stone into small pieces. The study of

physical phenomena such as movement of small solid dust particles in rocket exhaust, astrophysical problem and dust flow in geophysical problems is also very important. When a weak shock wave is propagated in a dusty gas flow with magnetic field then density, pressure, velocity and the energy carried by a weak shock wave changes across the shock and has a significant difference from those which arise when the weak shock wave passes through an ideal gas flow and dusty gas flow. Most of the physical phenomenon occuring in the nature are represented by quasilinear hyperbolic system of partial differential equations [110, 19]. In the nonlinear systems, the wave is considered as the moving surface along which the flow variables and their derivatives suffer certain kind of discontinuity that are carried along the surface. Further, the occurrence of these type of discontinuities are natural phenomenon in several physical situations like collision of galaxies, supernova explosions, space science, photo ionized gas, space re-entry vehicles, stellar winds and other astrophysical situations.

Dusty gas is considered to be mixture of gas and small solid dust particles where these dust particles attain less than five percent of total volume Miura [158]. At very high speed of fluid, these small solid particles behave as a pseudo fluid Pai [159]. Also, the study of evolutionary behaviour of shock wave in the mixture of gas and dust particles has grabbed more attention in many areas of industrial applications and space exploration such as collision of interplanetary objects, supersonic flights in polluted air, metallized propellant rocket, safe explosion into coal mines, under ground explosions, interstellar masses, explosive volcanic eruptions, movement of high speed vehicle in sand storms, application in space and other fields. Further, the presence of dust particle increases the shock formation distance Chaturvedi et al. [115].

The main motivation to work on magnetogasdynamics with dust particles is its application in Astrophysics as dusty plasmas are common in astrophysical environments;

examples range from the interstellar medium to cometary tails and planetary ring system. Where there are plasmas, there are charged particle zipping around and thus, there are magnetic fields. So the magnetic fields threading the planet and sun, the solar system, distant nebulas and even the galaxy itself. The change of the dust charge, when it is transferred from the region of weak magnetic field to the region of strong magnetic field can be used in many experiments. The change of dust charges by magnetic fields is important in dust shocks, in strong magnetic fields where the value of the magnetic field suddenly changes at the surface of the shock. The consideration of the mixture of an infinitely conducting gas and inert dust particles (obeying Pai's dusty gas model) as an infinitely conducting mixture may be a good approximation when the volume fraction of solid particles in the mixture is much smaller than that of the gas in the mixture. The magnetogasdynamic equations of motion can then be supposed to describe the flow of such a dusty gas in presence of a magnetic field. Consolmagno [160] has shown the influence of the Interplanetary Magnetic Field on Cometary and Primordial Dust Orbits. Morfill and Grün [161] described the motion in charged dust particles in interplanetary space.

Our main motive of the present work is to analyze the evolution of shock wave in magnetogasdynamic flow with dust particles. By using the method of progressive wave approach, the evolution of magnetic shock wave in mixture of gas and small solid dust particles has not been analyzed by anyone untill now. Though the problem has significant applications in many areas such as nuclear physics, plasma physics, geophysics and astrophysics etc. The propagation of shock wave in dusty gas flow with magnetic field is more complex natural phenomenon as compared to ideal gas flow. The investigation of asymptotic nature of non-linear wave propagation and its analysis have been discussed by using several approaches in different gaseous media. Using the ray method, Hunter [162] obtained the weakly nonlinear wave solution of quasilinear hyperbolic system. Choquet-Bruhat [58] considered the asymptotic

technique to analyze the weakly non-linear wave propagation in which they have determined the shockless solution of hyperbolic system. Most of the authors such as Fusco and Engelbrecht [39], Germain [163], Fusco [37], Sharma et. [40] and Singh et al. [118] have discussed weakly non-linear wave evolution in different gaseous media by using the progressive wave technique.

The problem of investigation of asymptotic behaviour of the governing system of quasilinear hyperbolic partial differential equations has got remarkable attention by many researchers. Singh et al. [118] have utilized the asymptotic technique to study the evolution of shock waves in magnetogasdynamic flow with radiation. Nandkeolyar et al. [143] have studied the hydromagnetic natural convection flow of a incompressible dusty fluid in the presence of transverse magnetic field and thermal radiation. Nath [164] investigated the evolution of shock wave in a rotational axisymmetric non-ideal gas flow with magnetic field. In last few decades, most of the authors have focussed on the shock related phenomenon in which they have analyzed the effect of dust particles in gas flow. Nath et al. [43] determined the influence of dust particles on the propagation of shock wave. Chaturvedi et al. [115, 165] analyzed the propagation of shock wave in planar and non-planar ideal gas flow in the presence of small solid particles. Nath [141] studied the evolution of exponential shock wave in non-ideal gas flow with small solid dust particles. By using the asymptotic technique, Gupta et al.[140] discussed the asymptotic behaviour of shock wave in non-ideal radiating gas flow. Nath [166, 167] obtained the self similar solution for one dimensional unsteady flow of dusty gas. Vishwakarma et al. [168] investigated the propagation of diverging cylindrical shock waves in a weakly conducting dusty gas (mixture of a perfect gas and small solid particles) under the influence of a spatially variable axial magnetic induction.

The main objective of the present work is to analyze the process of weak shock wave propagation in an inviscid, compressible, dusty gas under the influence of axial

magnetic field. By utilizing the weakly non-linear asymptotic technique, an equation governing the process of weak shock wave propagation in dusty gas flow with axial magnetic field has been derived. A Bernoulli type evolution equation is obtained here which determines the wave propagation phenomenon. The condition for time of first wave breaking for planar and non planar flow has been computed. We also derive equation governing the evolution of acceleration wave in a dusty gas flow in magnetogasdynamic regime. The shock relations for the weak shock wave have been derived which is utilized to compute the relations for the length(l) and velocity (v) profile of half N-wave for both the cases, non-planar and planar flow. Further, we present the results obtained graphically to analyze the effect of mass fraction of solid particles on the propagation of weak shock wave in magnetogasdynamic flow. Also, we analyze the effect of Alfven number on the evolutionary process of weak shock wave in the presence of small solid dust particles. Kumar [169] discussed about the particular solutions of cylindrical shock waves in magnetogasdynamics. Tao and Duan [170] have studied the effects of the dust size distribution on the shock wave in dusty plasma. Gupta et al. [171] have analyzed the interaction of waves in one-dimensional dusty gas flow. Nath et al. [172] have obtained the self-similar solution for the flow behind an exponential shock wave in a rotational axisymmetric non-ideal gas with magnetic field. An analysis of the ion temperature gradient driven mode solitary and shock waves in superthermal plasma is presented by Rehan et al. [173]. Formation of ion-acoustic shock waves and their propagation nature in a magnetized plasma in the presence of superthermal trapped electrons are investigated by Sultana [174]. Sahu [175] analyzed the shock wave propagation in perfectly conducting rotational axisymmetric two-phase medium with increasing energy under the action of heat conduction and radiation heat flux. Rehab M. and El-Shiekh [176] obtained the novel solitary and shock wave solutions for the generalized variable-coefficients (2+1)-dimensional KP-Burger equation arising in dusty plasma.

The present work is divided into sections as: In second section, we present the fundamental equations of motion and determine the characteristics of the governing system of PDEs. In third section, by applying the asymptotic expansions, we have determined the transport equation. Also, the conditions for first wave breaking have been derived. The analysis of previous section is utilized to discuss the evolutionary behaviour of acceleration wave in fourth section. In section fifth, Rankine-Hugoniot jump conditions are derived for weak shock wave in dusty gas flow with axial magnetic field. The shock relations derived in section fifth have been utilized to discuss the propagation of weak shock wave in the form of half N-wave and find the relations for length and velocity of saw-tooth profile in section six. The results obtained were computed and presented graphically to analyze the effect of small solid particles and axial magnetic field on the velocity and length of half N-wave. In the last section, the conclusion of the present work is given.

6.2 Governing equation

The fundamental equations for one dimensional unsteady motion of a dusty gas in the presence of a transverse magnetic field may be written as [177, 168],

$$\frac{\partial \rho}{\partial t} + \rho \frac{\partial v}{\partial r} + v \frac{\partial \rho}{\partial r} + \frac{\rho n v}{r} = 0, \tag{6.1}$$

$$\frac{\partial v}{\partial t} + v \frac{\partial v}{\partial r} + \frac{1}{\rho}\left(\frac{\partial p}{\partial r} + \frac{\partial h}{\partial r}\right) = 0, \tag{6.2}$$

$$\frac{\partial p}{\partial t} + v \frac{\partial \rho}{\partial r} + \rho C^2 \left(\frac{\partial v}{\partial r} + \frac{nv}{r}\right) = 0, \tag{6.3}$$

$$\frac{\partial h}{\partial t} + v \frac{\partial h}{\partial r} + 2h \left(\frac{\partial v}{\partial r} + \frac{nv}{r}\right) = 0, \tag{6.4}$$

where, ρ and p represent the fluid density and pressure respectively. t is the time, r is the spatial coordinate and v denotes fluid velocity. h is magnetic pressure defined as $h = \dfrac{\nu H^2}{2}$, where ν represents magnetic permeability and H is the transverse magnetic field which is axial in planar case ($n = 0$) and in the cylindrical case, the magnetic lines of force can be straight lines parallel to the axis of symmetry or concentric circles with centres on the axis of symmetry. The letter n will take value 0 for planar flow and value 1 for cylindrically symmetric flow.

The quantity C is the equilibrium speed of sound which can be written as

$$C = \left(\frac{\Gamma p}{\rho(1-\theta\rho)}\right)^{1/2}, \tag{6.5}$$

where, $\Gamma = \dfrac{\gamma(1+\lambda\beta)}{(1+\lambda\beta\gamma)}$, $\lambda = \dfrac{k_p}{(1-k_p)}$, $\beta = \dfrac{c_{sp}}{c_p}$, $\gamma = \dfrac{c_p}{c_v}$.

Here c_p and c_v denotes the specific heat of the gas at constant pressure and constant volume respectively and c_{sp} represent the specific heat of the solid particles.

The volume fraction Z is defined as,

$Z = \dfrac{V_{sp}}{V_g}$

and in the mixture, k_p is constant which represents the mass fraction of the solid particles which defined as,

$k_p = \dfrac{m_{sp}}{m_g}$.

Here, V_{sp} and m_{sp} represent the volumetric extension and the total mass of the solid particles respectively. V_g denotes the total volume and m_g denotes total mass of the mixture. The relation between Z and k_p are represented by the equation $Z = \theta\rho$, where θ is constant which is defined as $\theta = \dfrac{k_p}{\rho_{sp}}$, with ρ_{sp} being the species density of solid particles.

The equation of state is written as

$$p = \frac{(1-k_p)}{(1-Z)}\rho RT, \tag{6.6}$$

where, T and R are the temperature of the gas and gas constant respectively.

Now, the matrix form of system of equations (6.1) to (6.4) may be written as

$$\frac{\partial V}{\partial t} + M\frac{\partial V}{\partial r} + N = 0. \tag{6.7}$$

Here,

$$V = \begin{bmatrix} \rho \\ v \\ p \\ h \end{bmatrix}, M = \begin{bmatrix} v & \rho & 0 & 0 \\ 0 & v & \frac{1}{\rho} & \frac{1}{\rho} \\ 0 & \rho C^2 & v & 0 \\ 0 & 2h & 0 & v \end{bmatrix}, N = \begin{bmatrix} \frac{n\rho v}{r} \\ 0 \\ \frac{m\rho C^2 v}{r} \\ \frac{2hnv}{r} \end{bmatrix}. \tag{6.8}$$

The system of equation (6.7) can be written in the following form

$$V^i{}_t + M^{ij}V^j{}_r + N^i = 0, \qquad i,j = 1,2,3,4, \tag{6.9}$$

where, M^{ij} are components of matrix M. V^i and N^i are components of column vector V and N respectively.

The eigenvalues of the matrix M are given as

$$\lambda_1 = v - a, \;\; \lambda_2 = v, \;\; \lambda_3 = v, \;\; \lambda_4 = v + a. \tag{6.10}$$

Hence, system of equation (6.7) is hyperbolic.

Here, a is magneto-acoustic speed defined as

$$a = (C^2 + d^2)^{1/2} = \frac{\Gamma p}{\rho(1-\theta\rho)}\left(1 + \frac{d^2}{C^2}\right)^{1/2} = \frac{\Gamma p}{\rho(1-\theta\rho)}\mu^{1/2}, \tag{6.11}$$

where, $d = \left(\frac{2h}{\rho}\right)^{1/2}$ is the Alfven speed and $\mu = 1 + \frac{d^2}{C^2}$ is constant which represents Alfv́en number. The left and right eigenvector corresponding to the eigenvalue λ_4 of the matrix M are

$$l^T = \begin{bmatrix} 0 \\ \rho a \\ 1 \\ 1 \end{bmatrix}, k = \begin{bmatrix} 1 \\ \frac{a}{\rho} \\ C^2 \\ d^2 \end{bmatrix}, \tag{6.12}$$

where, superscript denotes transposition.

The following cases may arise on the dependence of the parameter Γ, θ and μ:

Case 1: When $\theta = 0$, $\mu = 1$ and $\Gamma = \gamma$ then $a^2 = \frac{\gamma p}{\rho}$. Hence mixture converts in an ideal gas.

Case 2: When $\theta = 0$, $\mu > 1$ and and $\Gamma = \gamma$ then $a^2 = \frac{\gamma p}{\rho}\mu^{1/2}$. Hence It becomes magnetogasdynamics flow without dust particles.

Case 3: When $\theta \neq 0$, $\mu = 1$ then $a^2 = \frac{\Gamma p}{\rho(1-\theta\rho)}$. Hence mixture converts in ideal gas with small solid dust particles.

Case 4: When $\theta \neq 0$, $\mu > 1$ then $a^2 = \frac{\Gamma p}{\rho(1-\theta\rho)}\mu^{1/2}$. It becomes the case of magnetogasdynamics flow with dust particles.

6.3 Progressive Wave Solutions

By applying the asymptotic expansion, we obtained the asymptotic solution of (6.7) which exhibits the characterization of progressive waves. Now, an asymptotic expansion for V^i is written as

$$V^i(x,t) = V_0^i + \epsilon V_1^i(r,t,\psi) + O(\epsilon^2). \tag{6.13}$$

Here, V_0^i is known constant solution of Eq.(6.7) with $N^i(V_0) = 0$ and all the remainning terms in Eq.(6.1) exhibits the character of progressive waves. ϵ is small parameter which depends upon the physical problem to be studied. The magnitude of ϵ depends on the physical problem which is considered here. The parameter ϵ is ratio of characteristics time scale of medium (τ_{chr}) and attenuation time (τ_{at}) such that $\epsilon = \tau_{ch}/\tau_a \ll 1$. The variable ψ is known as "fast variable" defined by $\psi = F(r,t)/\epsilon$, where $F(r,t)$ determined the wavefront and it is known as phase function. It is noticed here that the situation $\tau_{chr} \ll \tau_a$ i.e. characteristics time scale of medium is very small as compared to attenuation time which is corresponding to the propagation of high frequency wave [130].

Now, by using the asymptotic expansion from Eq.(6.13) and applying the Taylor's series expansion for M^{ij} and N^i in the neighbourhood of V_0^i(uniform solution), we obtained

$$M^{ij} = M_0^{ij} + \epsilon \left(\frac{\partial M^{ij}}{\partial V^k}\right)_0 V_1^k + O(\epsilon^2), \tag{6.14}$$

$$N^i = N_0^i + \epsilon \left(\frac{\partial N^i}{\partial V^k}\right)_0 V_1^k + O(\epsilon^2). \tag{6.15}$$

Hence, by utilizing the Eq.(6.13) to (6.15) in (6.9) and equating to zero the coefficient of ϵ^0 and ϵ^1, we obtained

$$\left(M_0^{ij} - \lambda \delta_j^i\right) \frac{\partial V_1^j}{\partial \psi} = 0, \tag{6.16}$$

$$\left(M_0^{ij}-\lambda\delta_j^i\right)\frac{\partial V_2^j}{\partial\psi}+\left(\frac{\partial V_1^i}{\partial t}+M_0^{ij}\frac{\partial V_1^j}{\partial r}\right)F_r^{-1}+V_1^k\left(\frac{\partial M^{ij}}{\partial V^k}\right)_0\frac{\partial V_1^j}{\partial\psi}+F_r^{-1}V_1^k\left(\frac{\partial N^i}{\partial V^k}\right)_0=0. \tag{6.17}$$

Here, $\lambda=-F_t/F_r$ and δ_j^i is defined as Krönecker delta. The subscript 0 represents that the quantity associated is determined at constant state V_0. With the help of Eq.(6.16), characteristics polynomial is obtained as $\lambda^2(\lambda^2-a_0^2)=0$, giving the eigen values of M_0 as $\pm a_0\neq 0$. From Eq. (6.12), the left and right eigenvectors with respect to eigen value $\lambda=a_0$ of matrix M_0 are given by

$$l^T=\begin{bmatrix}0\\ \rho_0 a_0\\ 1\\ 1\end{bmatrix},k=\begin{bmatrix}1\\ a_0/\rho_0\\ C_0^2\\ d_0^2\end{bmatrix}. \tag{6.18}$$

By Eq.(6.16), we analyzed that $\dfrac{\partial V_1}{\partial\psi}$ is collinear to k_0, therefore V_1 can be represented as

$$V_1(r,t,\psi)=P(r,t,\psi)k_0+\Omega(r,t). \tag{6.19}$$

Eq.(6.19) determines the solution of Eq.(6.17), where $P(x,t,\psi)$ is known as amplitude factor to be calculated letter. Ω^i are constants of integration which are components of the vector Ω and these are not of the nature of progressive wave, therefore it may be neglected. Further, the phase function i.e. $F(r,t)$ may be written as

$$F_t+a_0F_r=0, \tag{6.20}$$

and if $F(r,0)=r-r_0$, then

$$F(r,t)=(r-r_0)-a_0t. \tag{6.21}$$

Hence, by multiplying Eq.(6.17) with l^i and utilizing Eq.(6.21) in resulting equation we obtained the following equation for P, which is used to analyze the evolution of the disturbance

$$\frac{\partial P}{\partial \tau} + A_0 P \frac{\partial P}{\partial \psi} + B_0 P = 0, \tag{6.22}$$

where $\frac{\partial}{\partial \tau} = \frac{\partial}{\partial t} + a_0 \frac{\partial}{\partial r}$, is the ray derivative which is taken along the ray direction. Here

$$A_0 = k_0^m \left(\frac{\partial (v+a)}{\partial V^m} \right)_0 = \frac{(\Gamma+1) C_0^2}{2\rho_0 a_0 (1 - Z_0)} + \frac{3}{2} \frac{d_0^2}{\rho_0 a_0} > 0, \tag{6.23}$$

$$B_0 = (l_0^i k_0^i)_0^{-1} \left((l_0^j r_0^k) \frac{\partial N^i}{\partial V^m} \right)_0 = \frac{n a_0}{2r}, \tag{6.24}$$

where, B_0^{-1} has dimension of time and it can be taken as consisting of attenuation time τ_{at} determining the medium. Further, we obtained that Eq.(6.22) is hyperbolic partial differential equation and its characteristics curve can be written as:

Case I: For planar flow ($n = 0$)

$$\psi = \psi_0 + \tau A_0 \eta(r_0, \psi_0). \tag{6.25}$$

Case II: For cylindrically symmetric flow ($n = 1$),

$$\psi = \psi_0 + 2A_0 \eta(r_0, \psi_0) \frac{r_0}{a_0} \left[\left(\frac{r_0 + a_0 \tau}{r_0} \right)^{1/2} - 1 \right]. \tag{6.26}$$

Here, $\eta(r_0, \psi_0) = P|_{\tau=0}$, $\psi_0 = \frac{F|_{\tau=0}}{\epsilon}$ and $r = r|_{\tau=0}$. Further, we ensure about the formation of shock wave by the Eq.(6.25) and Eq.(6.26) which provides the existence of an envelope of characteristics curves. From above discussion it is clear that the shock formation is confirmed for only those characteristics which satisfy the condition $\tau > 0$, i.e. $\frac{\partial \eta}{\partial \psi_0} < 0$. The time of shock formation for planar and cylindrical compressive waves can be obtained as

Case I: For planar wave ($n = 0$),

$$\tau_{shf} = min\left[A_0|\frac{\partial \eta}{\partial \psi_0}|\right]^{-1}. \tag{6.27}$$

Case II: For cylindrically symmetric wave($n = 1$),

$$\tau_{shf} = min\left(\frac{r_0}{a_0}\left[\left(\frac{a_0 + 2r_0A_0|\frac{\partial \eta}{\partial \psi_0}|}{2r_0A_0|\frac{\partial \eta}{\partial \psi_0}|}\right)^2 - 1\right]\right). \tag{6.28}$$

Here, the minimum value is determined on a suitable domain of the quantities r_0 and ψ_0.

6.4 Acceleration Waves

By using the above analysis, we analyze the acceleration waves for the governing system of Eqs. (4.12) to (4.15). We consider that the acceleration front is denoted by the curve $F(r, t) = 0$, across which the velocity is continuous but it's first and higher order derivatives admit jump discontinuities. Further, in the neighbourhood of the acceleration front the velocity v can be expressed by the expansion

$$v = \epsilon v_1(r, t, \psi) + O(\epsilon^2). \tag{6.29}$$

Here $v_1 = 0$ for $\psi < 0$ and $v_1 = O(\psi)$ for $\psi > 0$. With the help of Eq.(6.13), we obtained that v_1 is an element of column vector V_1. Therefore, we have

$$P(r, t, \psi) = \begin{cases} 0, & \text{if } \psi < 0, \\ \psi\alpha(r, t) + O(\psi^2), & \text{if } \psi > 0, \end{cases} \tag{6.30}$$

where $\alpha = \left(\frac{a_0}{c_0}\omega\right)$ with $\omega = \left[\frac{\partial v}{\partial r}\right]$, denotes the jump in velocity gradient across the acceleration front.

Further, with the help of Eq.(6.22) and Eq.(6.30) at the front $\psi = 0$, the resulting equation becomes Bernoulli-type ordinary differential equation which can be written in the following form

$$\frac{d\omega}{dt} + B_0\omega + \Lambda_0\omega^2 = 0. \tag{6.31}$$

Here, $\Lambda_0 = \frac{1}{2\mu}\left(\Gamma(1+Z_0) + 3\mu + Z_0 - 2\right)$ and $B_0 = \frac{na_0}{2r}$.

The solution of ordinary differential equation Eq.(6.31) is obtained as

Case I: For planar flow ($n = 0$),

$$\omega = \frac{w_0}{(1 + w_0\Lambda_0 t)}. \tag{6.32}$$

Case II: For cylindrically symmetric flow ($n = 1$),

$$\omega = \frac{\omega_0}{\left(1 + \frac{a_0 t}{r_0}\right)^{1/2}\phi}, \tag{6.33}$$

where, $\phi = \left[1 + \frac{2\Lambda_0}{a_0 r_0\left(\left(1 + \frac{a_0 t}{r_0}\right)^{1/2} - 1\right)\omega_0}\right]$ and $\omega_0 = \omega|_{t=0}$.

6.5 Weak shock

With the help of previous analysis, it is obvious that in the beginning compression pulse may be weak but after a finite time it culminates into a shock wave. The flow and field variables before the shock wave and after the shock wave are denoted by

the subscript 0 and subscript $*$ respectively. These flow and field variables satisfy the R-H jump condition for magnetogasdynamic flow with dust particles, written as

$$\rho_* = \rho_0(1+\delta), v_* = \frac{\delta U}{(1+\delta)}, p_* = p_0 + \frac{\delta}{(1+\delta)}\rho_0 U^2 - h_0\delta(2+\delta), h_* = h_0(1+\delta)^2. \tag{6.34}$$

Here, $\delta = \dfrac{(\rho_* - \rho_0)}{\rho_0}$, represents the shock strength parameter and U represents the the shock velocity. The shock strength parameter (δ) and shock velocity (U) are related by

$$U^2 = \frac{2(1+\delta)\left[C_0^2 + d_0^2\left((1-Z_0\delta)(1+\frac{\delta}{2}) - \frac{(\Gamma-1)\delta}{2}(1+Z_0)\right)\right]}{2(1-Z_0\delta) - \delta(\Gamma-1)(1+Z_0)}, \tag{6.35}$$

where, $Z_0 = \theta\rho_0$.

Hence , $\delta \ll 1$ for weak shock wave. Therefore, by the first approximation of Eq.(6.35) we obtained
$U = a_0\left(1 + \dfrac{\delta\Lambda_0}{2}\right)$. Subsequently, Eq. (6.34) yield the first approximation as

$$\rho_* = \rho_0(1+\delta), v_* = a_0\delta, p_* = p_0(1+\Gamma\delta(1+Z_0)), h_* = h_0(1+2\delta). \tag{6.36}$$

6.6 Decay of progressive wave in the form of half N-wave (sawtooth profile)

In this section, we determined the velocity and length of sawtooth wave (half N-wave). By traveling a long distance from the body moving with supersonic speed, sawtooth wave is originated Whitham[19]. Hence, sawtooth wave becomes sufficiently weak in the beginning therefore one may apply the R-H jump relation from Eq.(6.36) Zierep [33]. Further, we analyze the advancement of disturbance in the

shape of sawtooth wave (half N-wave) which is represented in Fig.1.

The left segment of sawtooth wave was situated initially at point r_0 and travels with magnetosonic speed a_0 in the medium at rest and right segment of sawtooth wave was placed initially at point r_{s0} moves faster. In the beginning, let us suppose that l_0 is the length of sawtooth wave (half N-wave). By suppressing the subscript $*$, let us represent v and a by the state at the rear side of the shock wave which is placed at time t as:

$$r_s(t) = r_0 + a_0 t + l(t),$$

where, at any time t, $l(t)$ denotes the length of the sawtooth wave (half N-wave). Hence,

$$U = \frac{dr_s}{dt} = a_0 + \frac{dl}{dt}. \tag{6.37}$$

Further, with the help of Eq.(6.36) we obtain

$$U = a_0 + \frac{v\Lambda_0}{2}. \tag{6.38}$$

The particle velocity v at the rear of the weak shock heading the sawtooth profile (half N-wave) can be expressed as [33]:

$$v = l(t)\omega, \tag{6.39}$$

where, $\omega = \left(\frac{\partial v}{\partial r}\right)_{r-r_0=a_0 t}$, represents the slope of half N-wave(sawtooth wave) at any time t which is obtained by Eq.(6.32) and (6.33).

Now, with the help of Eq.(6.38) and Eq.(6.39) and comparing the resulting expression with Eq.(6.37), we have

$$\frac{dl}{dt} = \frac{\omega l \Lambda_0}{2}. \tag{6.40}$$

It is noticed here that ω_0, l_0 and U_0 denote the value of ω, l and U at time $t = 0$ respectively. Also, by solving the Eq.(6.38) and Eq.(6.39) at time $t = 0$, we obtained

$$\omega_0 = \frac{2(U_0 - a_0)}{l_0 \Lambda_0}. \tag{6.41}$$

Hence, with the help of Eq.(6.40), Eq.(6.32) and Eq.(6.33) we get the length of half-N wave.

Case I: For planar flow ($n = 0$),

$$\frac{l}{l_0} = (1 + \omega_0 \Lambda_0 t)^{1/2}. \tag{6.42}$$

Case II: For cylindrically symmetric flow ($n = 1$),

$$\frac{l}{l_0} = \left[1 + \frac{2\Lambda_0}{a_0 r_0 \left(\left(1 + \frac{a_0 t}{r_0}\right)^{1/2} - 1\right)\omega_0}\right]^{1/2}. \tag{6.43}$$

By utilizing Eq.(6.32) and Eq.(6.33) and substituting in Eq.(6.40), the velocity of sawtooth wave (half-N wave) can be written as:

Case I: For planar flow ($n = 0$),

$$\frac{v}{v_0} = (1 + \omega_0 \Lambda_0 t)^{-1/2}. \tag{6.44}$$

Case II: For cylindrically symmetric flow ($n = 1$),

$$\frac{v}{v_0} = \left(\frac{r_0}{r_0 + a_0 t}\right)^{1/2} \left[1 + \frac{2\Lambda_0}{a_0 r_0 \left(\left(1 + \frac{a_0 t}{r_0}\right)^{1/2} - 1\right)\omega_0}\right]^{-1/2}, \tag{6.45}$$

where, $v_0 = v|_{t=0}$ i.e. value of v which is determined at $t = 0$.

6.7 Results and discussion

In the present study, we discuss the growth and decay of half N-wave (sawtooth wave) for different values of dusty gas parameters and axial magnetic field. The effect of small solid particles and axial magnetic field present in the solution appear through the parameters k_p, β and μ. Eq.(6.42) represents the length and Eq.(6.45) represents velocity of half N-wave (sawtooth wave) for planar and non-planar case. Let us consider two cases to explain about the solution, the first one is planar case and another one is cylindrically symmetric case. The velocity and length profile for half N-wave are depicted in Figure 2 to 9. The values of constants r_0, l_0, U_0 and ω_0 are taken as 1 in calculations. Also, for case $k_p = 0$ and $\beta = 0.0$, i.e. in the absence of small solid particles the results are in close agreement with earlier results [40].
Figure 2 and 3 denote the variation of length of half N-wave for planar flow under the influence of axial magnetic field and small solid particles. From Figure 2(a), it is observed that the effect of mass fraction of solid particles(k_p) decreases the length of sawtooth wave (half N-wave). Further, it is obtained here that the influence of increasing values of k_p is to slow down the decay of sawtooth profile which is due to, when a discontinuity passage through the dusty gas, the process of decay is slowed down by the particles(dust particles) of large inertia. Also, the presence of the dust particle in the medium contribute to shock strength. Figure 2(b) represents the effect of β (ratio of specific heat of solid particles and specific heat of gas at constant pressure) on the length of sawtooth wave (half N-wave) for planar case. The effect of increasing value of β is to further decrease the length of half N-wave i.e. it will slow down the decay process. From Figure. 2(a) and 2(b), it is noticed here that the

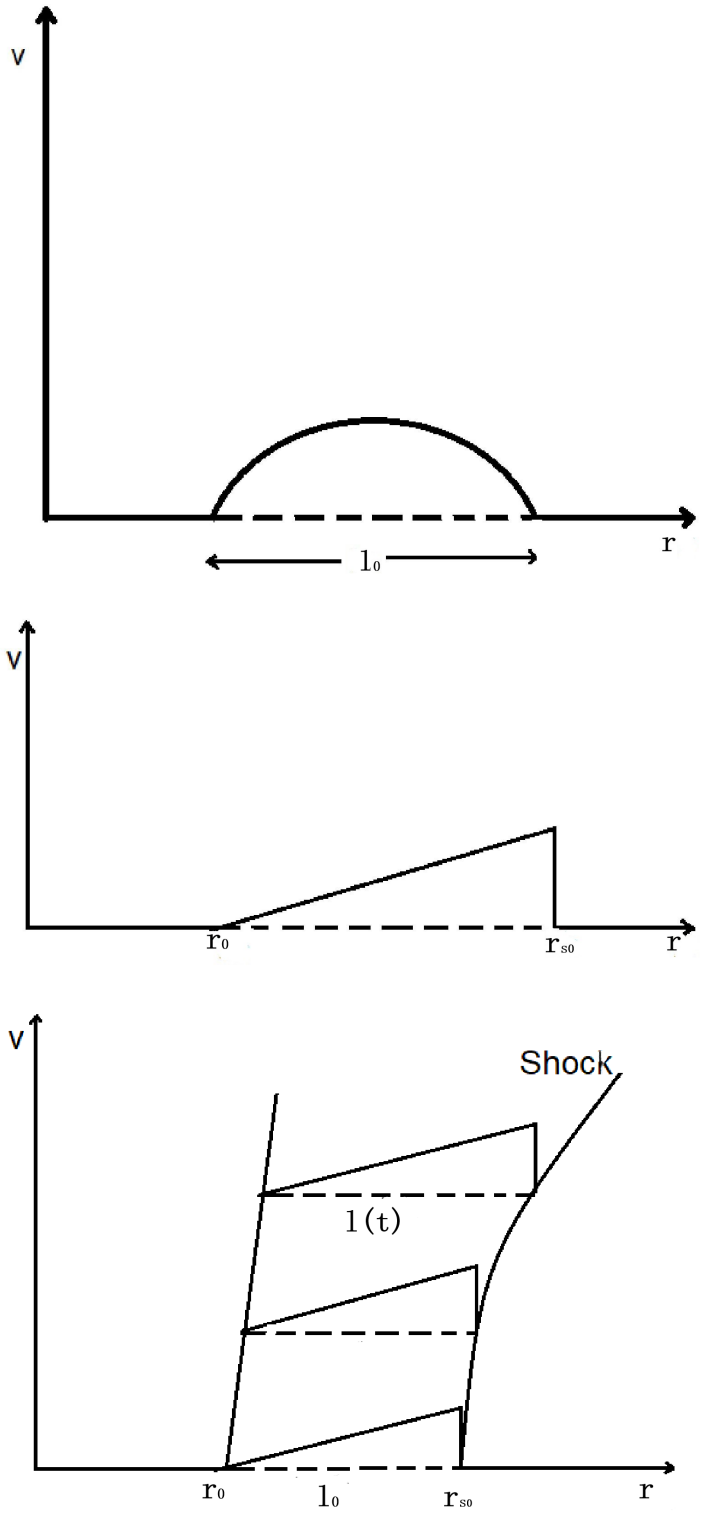

FIGURE 6.1: Formation and decay of Sawtooth wave (Half N-wave)

influence of k_p is to slow down the decay process of shock wave faster in comparison to the case of β. Figure.3 depicts the variation of length of half N-wave under the effect of mass fraction of solid particles and axial magnetic field for planar case. The increasing value of magnetic field enhances the length of sawtooth profile. It is clear that the effect of axial magnetic field causes to increase the growth rate of sawtooth wave (Half N-wave) as compared to in the absence of magnetic field ($\mu = 1.0$), i.e. it will increase the decay process of shock wave. It is analyzed here that the influence of mass fraction of solid particles (k_p) causes to slow down the decay process faster in the presence of axial magnetic field. Further, we obtained that under the coupling effect of dusty gas and axial magnetic field the decaying process of shock wave is slowed down in comparison to ideal gas. Figure.4 and Figure.5 depict the influence of k_p, β and μ on the length of half N-wave for cylindrically symmetric flow. Hence, it is analyzed here that the decay process of sawtooth wave (Half N-wave) enhances with respect to time in case of planar symmetry as compared to cylindrically symmetric flow.

Figure.6 and 7 denote the the variation of velocity of sawtooth wave for planar case under the influence of axial magnetic field and small solid particles. From Figure 6(a), it is observed that the effect of mass fraction of solid particles(k_p) increases the velocity of sawtooth wave. It is noticed here that the influence of increasing values of k_p is to slow down the decay of sawtooth profile. Figure 6(b) represents the effect of β (ratio of specific heat of solid particles and specific heat of gas at constant pressure) on the velocity of half N-wave for planar symmetry. The effect of increasing values of β is to further increase the velocity of half N-wave, i.e. it will slow down the decay process. From Figures. 6(a) and 6(b), it is noticed here that the influence of k_p is to slow down the decay process of shock wave faster in comparison to the case of β. Figure.7 depicts the variation of velocity of half N-wave under the effect of mass fraction of solid particles and axial magnetic field for planar case. The

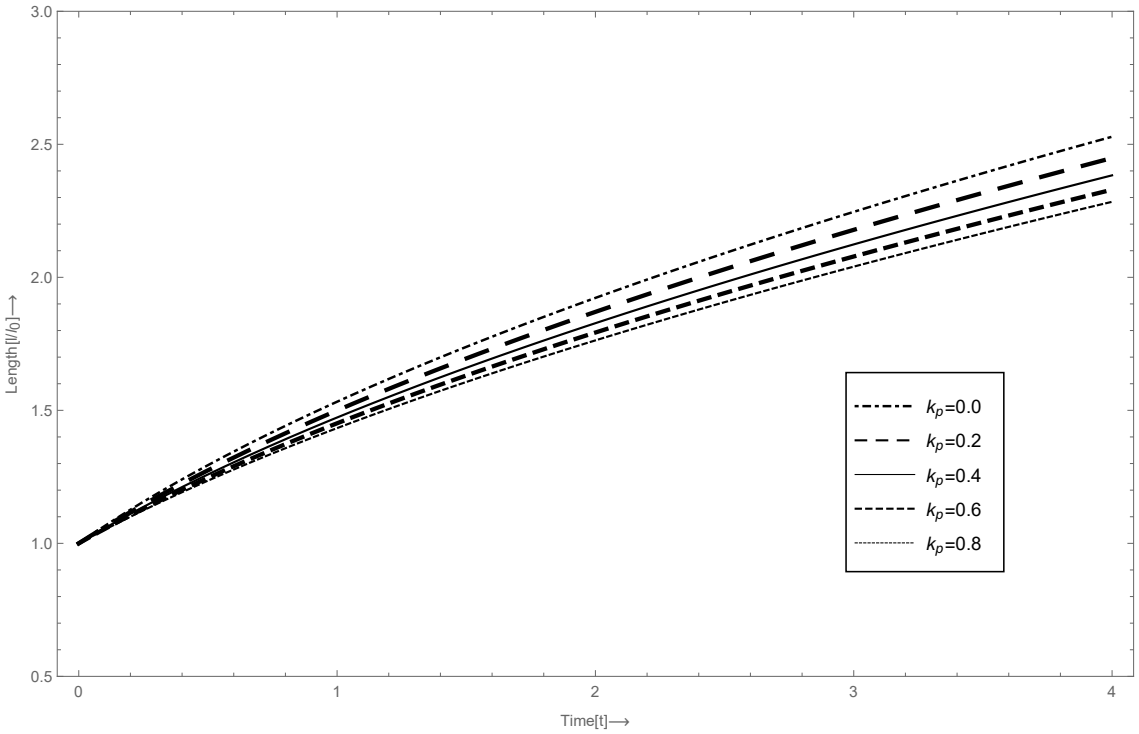

FIGURE 6.2: Variation of Length of sawtooth profile (l/l_0) for different value of mass fraction of solid particles (k_p) and time(t) with $\gamma = 1.67$, $\beta = 1.0$, $Z_0 = 0.01$ and $\mu = 1.0$ for planar flow.

increasing values of axial magnetic field decreases the velocity of sawtooth profile. It is clear that the effect of axial magnetic field causes to increase the growth rate of sawtooth wave (Half N-wave) as compared to in the absence of axial magnetic field ($\mu = 1.0$), i.e. it will increase the decay process of shock wave. It is analyzed here that the influence of mass fraction of solid particles (k_p) causes to slow down the decay process faster in the presence of axial magnetic field. Further, the influence of axial magnetic field causes to slow down the decay process in the presence of mass fraction of solid particles (k_p). Figures. 8 and 9 represent the variation of velocity of sawtooth wave (Half N-wave) for cylindrically symmetric flow under the influence of axial magnetic field and small solid particles. It is observed here that the velocity of sawtooth wave (Half N-wave) decreases faster with respect to time in non-planar flow in comparison to planar flow.

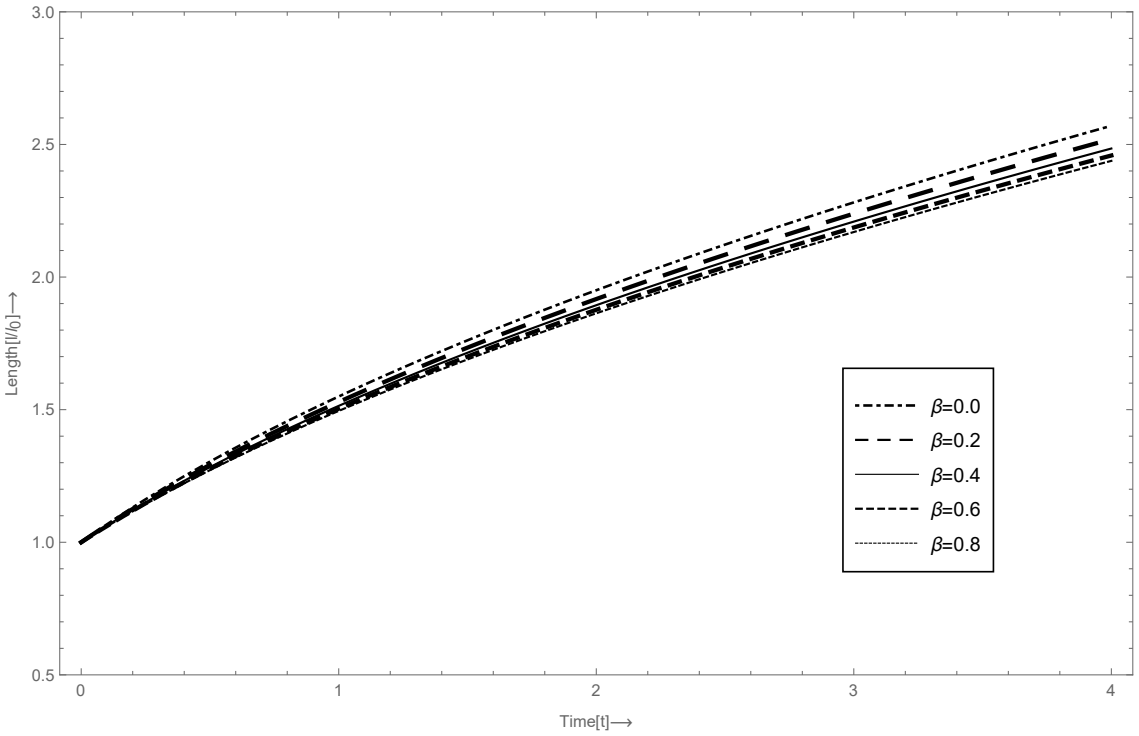

FIGURE 6.3: Variation of Length of sawtooth profile (l/l_0) for different value of β and time(t) with $\gamma = 1.67$, $k_p = 0.4$, $Z_0 = 0.01$ and $\mu = 1.0$ for planar flow.

6.8 Conclusion

In the present study, the method of progressive wave approach is utilized to investigate the asymptotic solution of weakly non-linear wave moving in an inviscid, compressible magnetogasdynamic flow with small solid particles. Also, we analyze the effect of mass fraction of solid particles (k_p), ratio of specific heat of solid particles and specific heat of gas at constant pressure (β) and axial magnetic field (μ) on the evolution of sawtooth wave (Half N-wave) for planar flow and cylindrically symmetric flow. Under the combined effect of axial magnetic field and small solid particles (dusty gas), the length and velocity for shock wave is analyzed. For determining the evolution of disturbance in high frequency domain, an evolution equation is derived here. Further, the condition for time of first wave breaking for planar and non planar flow has been computed. It is observed here that the presence of mass

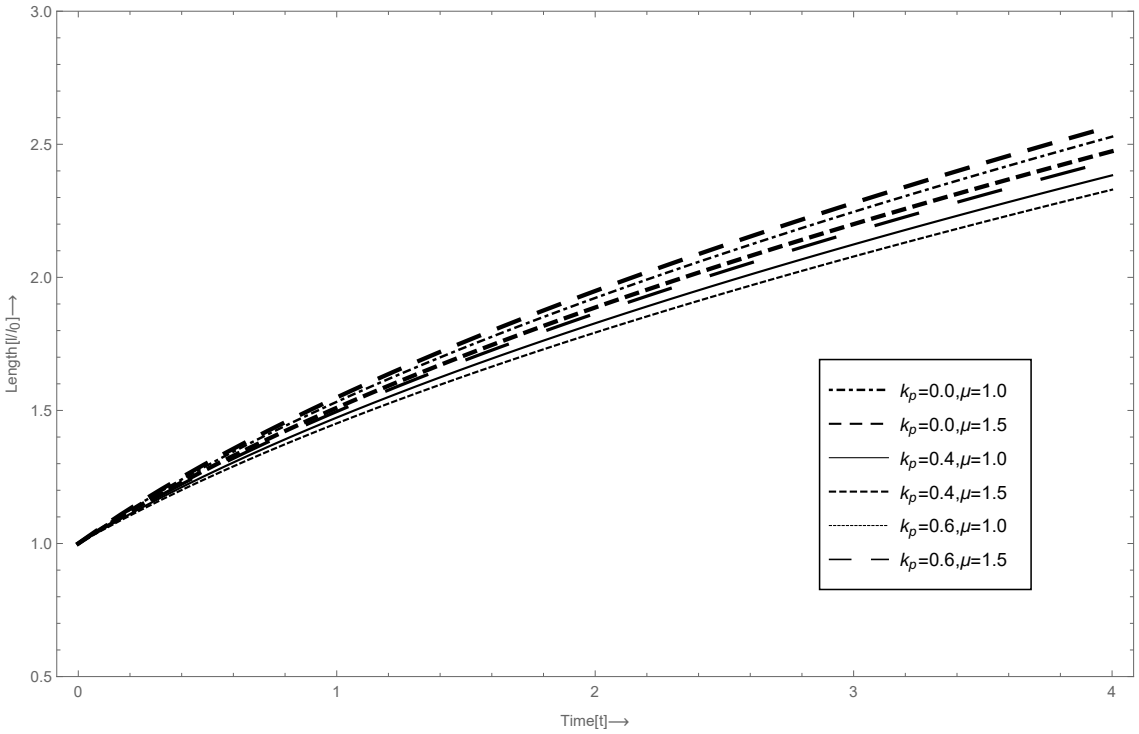

FIGURE 6.4: Variation of Length of sawtooth profile (l/l_0) for different value of k_p and μ with respect to time(t) with $\gamma = 1.67$, $Z_0 = 0.01$, and $\beta = 1.0$ for planar flow.

fraction of solid particles (k_p) and β both causes to slow down the decay process since the presence of the dust particle in the medium contribute to shock strength. Also, it is obtained that the effect of axial magnetic field causes to increase the growth rate of sawtooth wave (Half N-wave) as compared to in the absence of axial magnetic field. The effect of axial magnetic field causes to slow down the decay process in the presence of mass fraction of solid particles (k_p). Further, it is observed here that the decay process of sawtooth wave (Half N-wave) enhances with respect to time in case of planar flow as compared to cylindrically symmetric flow.

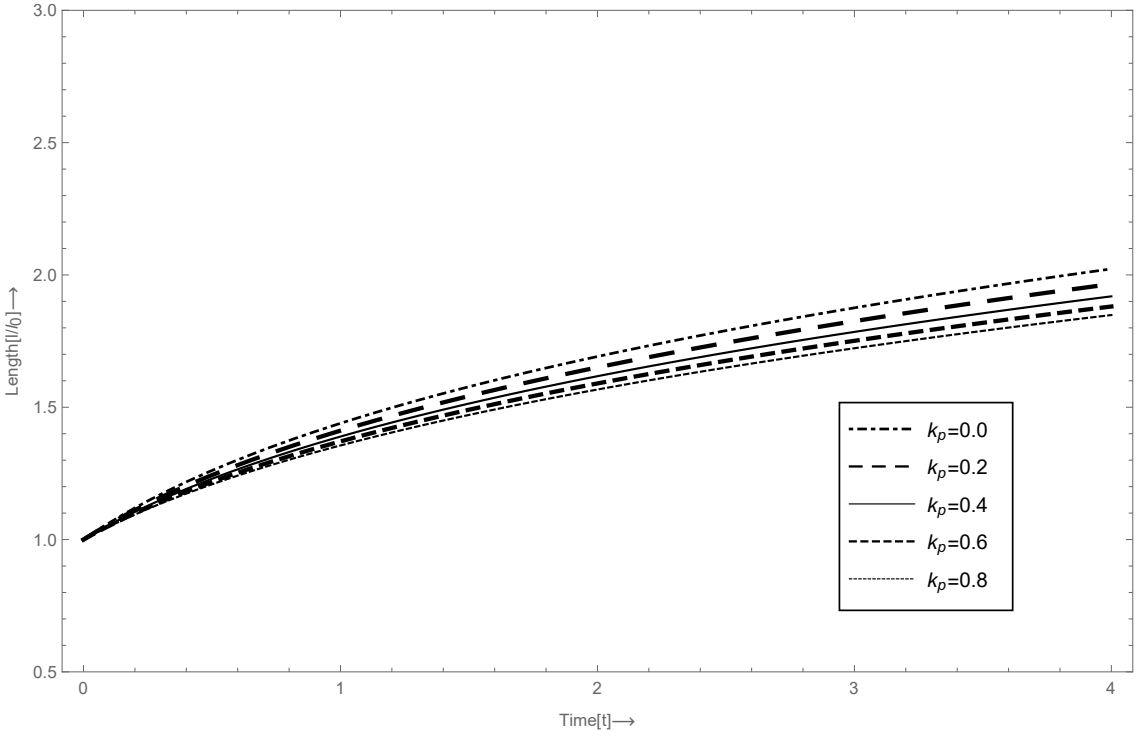

FIGURE 6.5: Variation of Length of sawtooth profile (l/l_0) for different value of mass fraction of solid particles (k_p) and time(t) with $\gamma = 1.67$, $\beta = 1.0$, $Z_0 = 0.01$ and $\mu = 1.0$ for cylindrically symmetric flow.

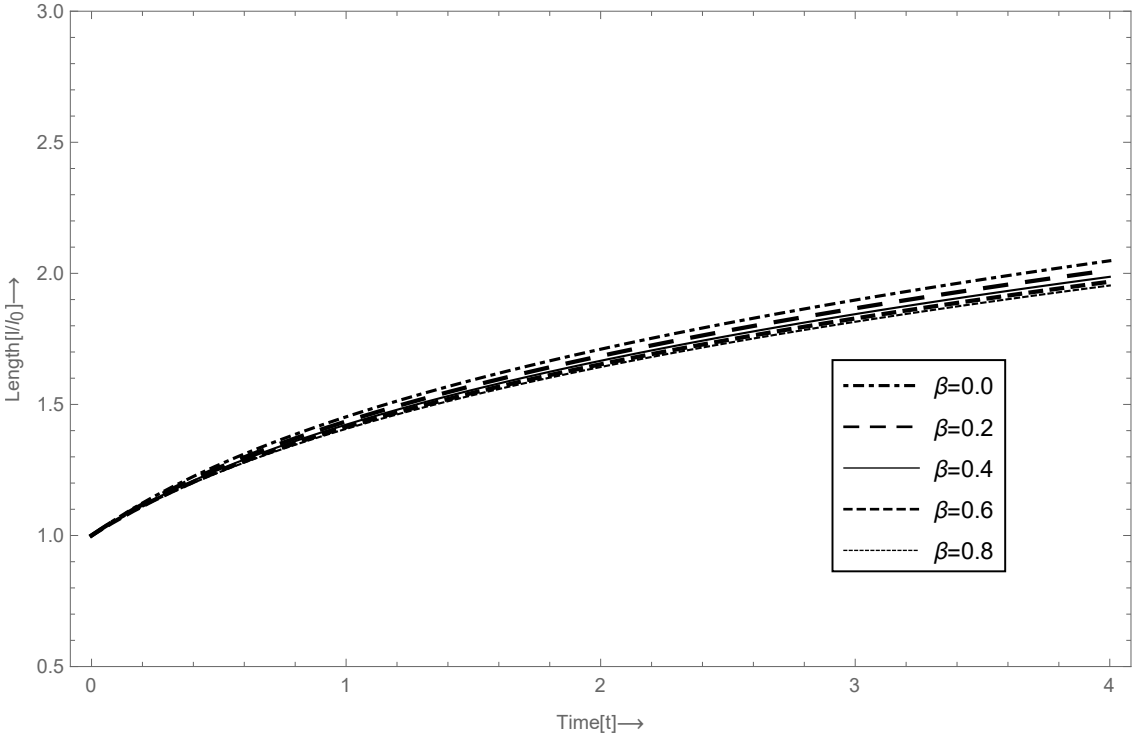

FIGURE 6.6: Variation of Length of sawtooth profile (l/l_0) for different value of β and time(t) with $\gamma = 1.67$, $k_p = 0.4$, $Z_0 = 0.01$ and $\mu = 1.0$ for cylindrically symmetric flow.

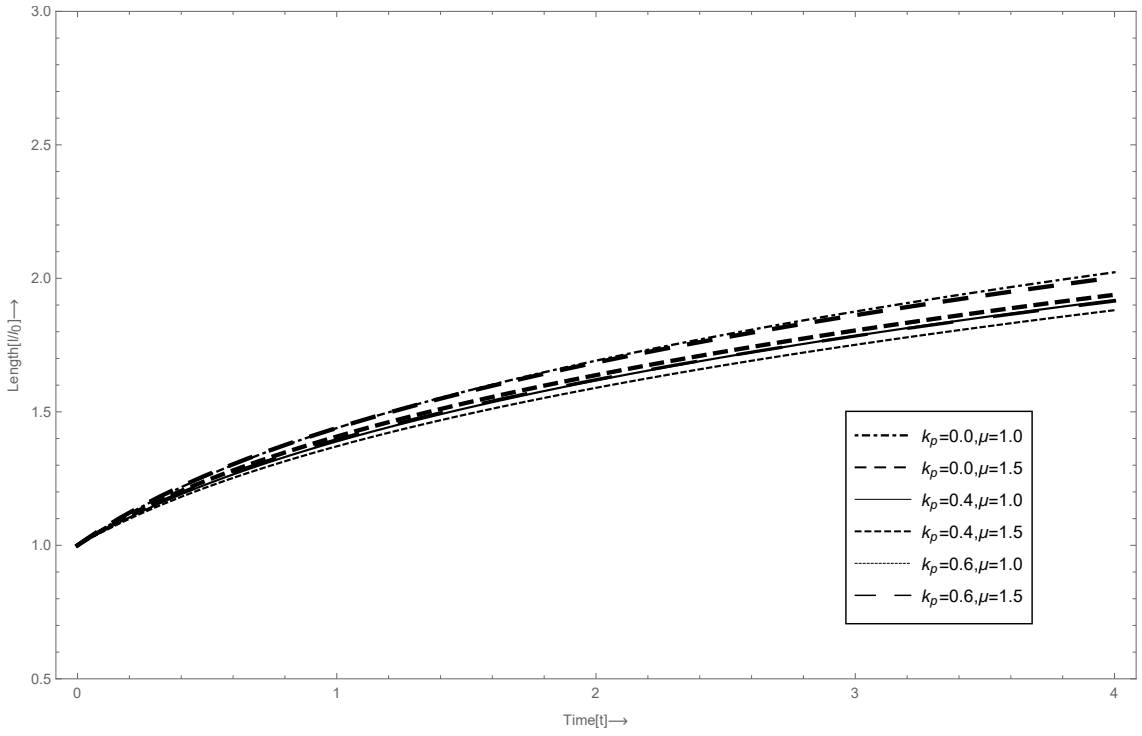

FIGURE 6.7: Variation of Length of sawtooth profile (l/l_0) for different value of k_p and μ with respect to time(t) with $\gamma = 1.67$, $Z_0 = 0.01$, and $\beta = 1.0$ for cylindrically symmetric flow.

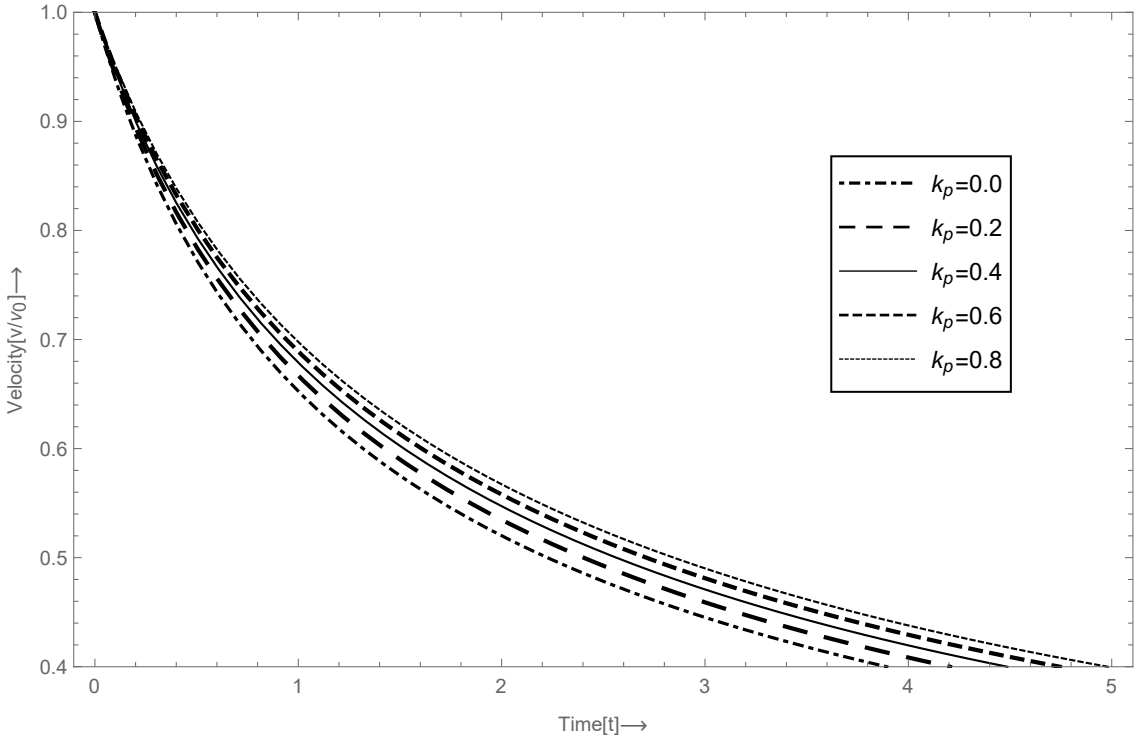

FIGURE 6.8: Variation of Velocity of sawtooth profile (v/v_0) for different value of mass fraction of solid particles (k_p) and time(t) with $\gamma = 1.67$, $\beta = 1.0$, $Z_0 = 0.01$ and $\mu = 1.0$ for planar flow.

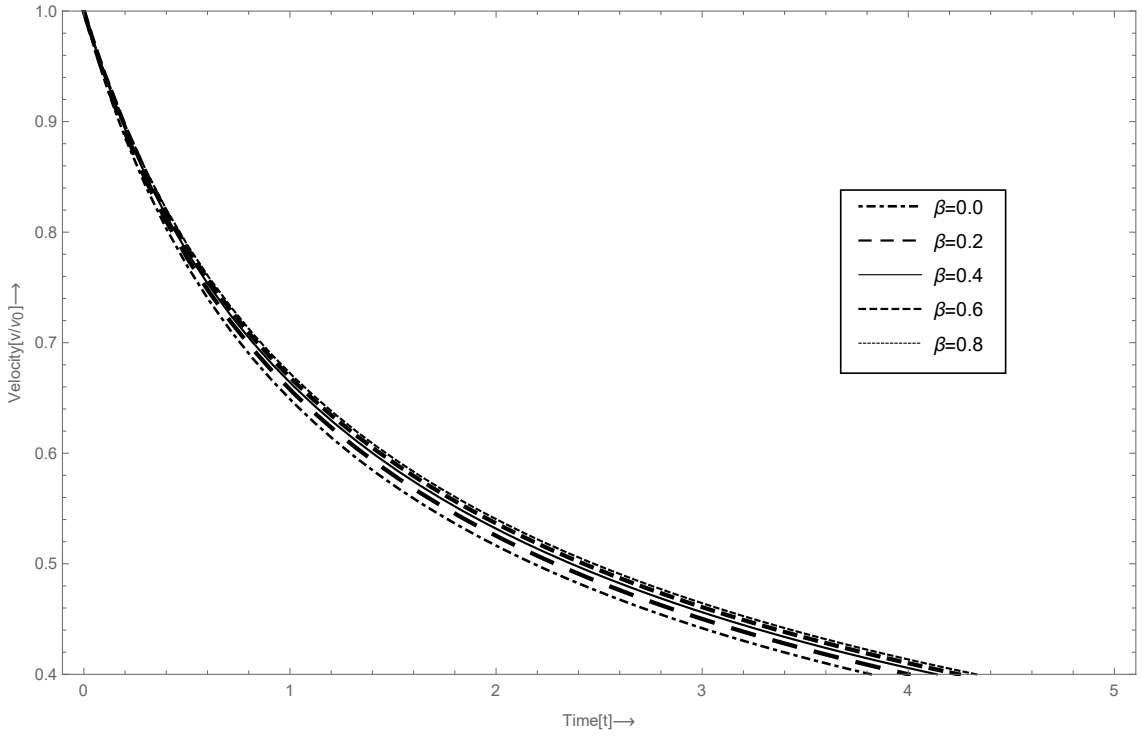

FIGURE 6.9: Variation of Velocity of sawtooth profile (v/v_0) for different value of β and time(t) with $\gamma = 1.67$, $k_p = 0.4$, $Z_0 = 0.01$ and $\mu = 1.0$ for planar flow.

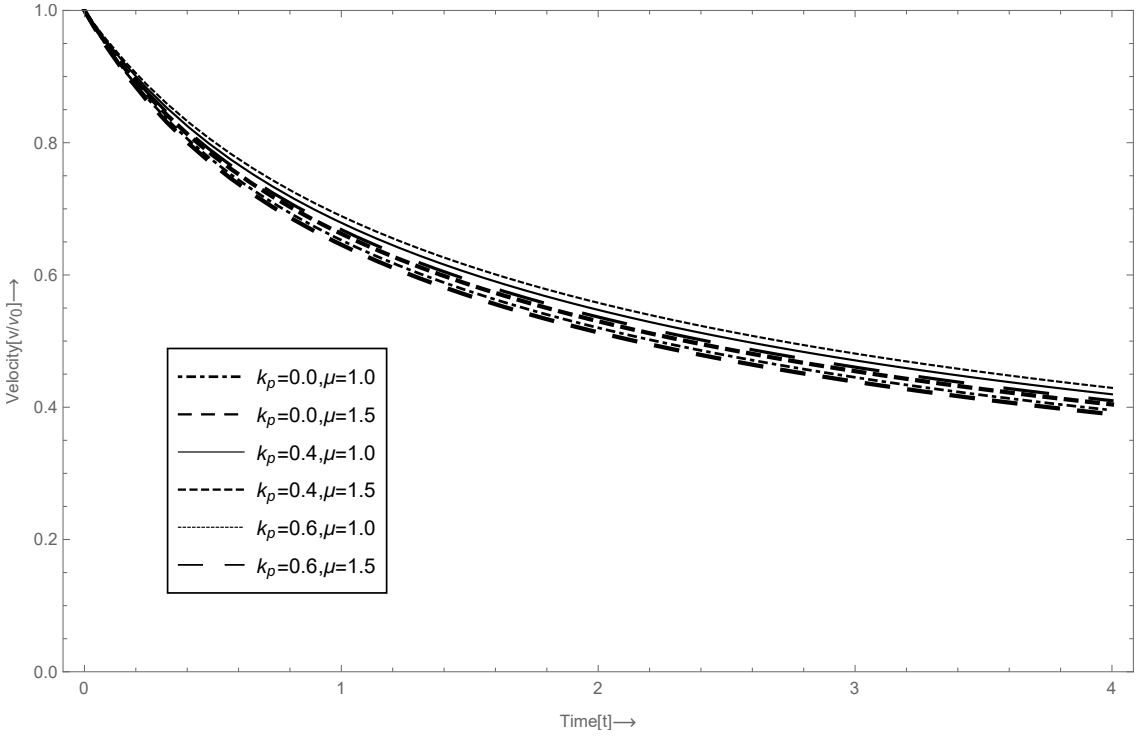

FIGURE 6.10: Variation of Velocity of sawtooth profile (v/v_0) for different value of k_p and μ with respect to time(t) with $\gamma = 1.67$, $Z_0 = 0.01$, and $\beta = 1.0$ for planar flow.

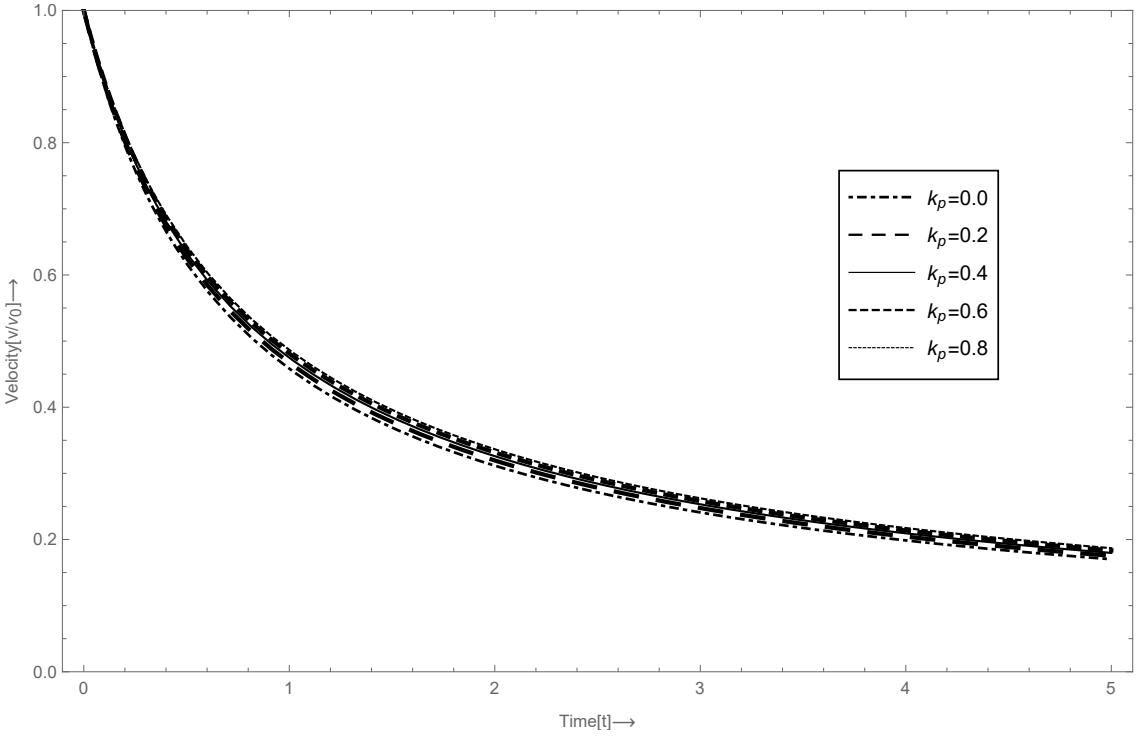

FIGURE 6.11: Variation of Velocity of sawtooth profile (v/v_0) for different value of mass fraction of solid particles (k_p) and time(t) with $\gamma = 1.67$, $\beta = 1.0$, $Z_0 = 0.01$ and $\mu = 1.0$ for cylindrically symmetric flow.

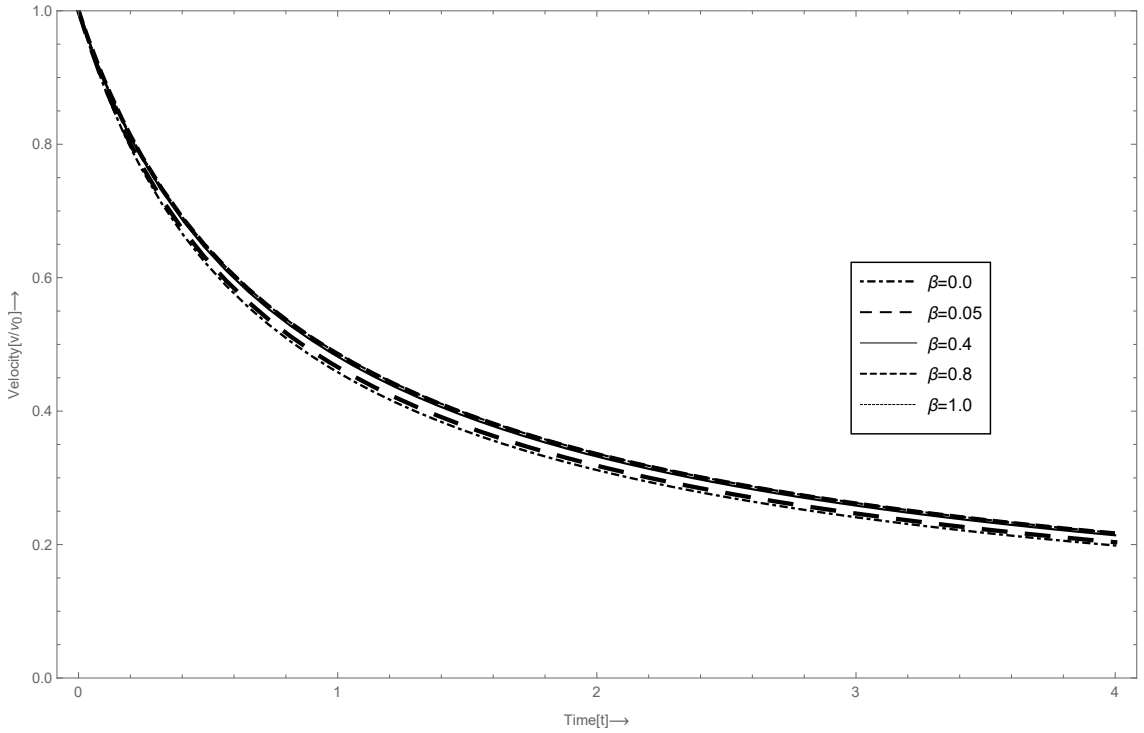

FIGURE 6.12: Variation of Velocity of sawtooth profile (v/v_0) for different value of β and time(t) with $\gamma = 1.67$, $k_p = 0.4$, $Z_0 = 0.01$ and $\mu = 1.0$ for cylindrically symmetric flow.

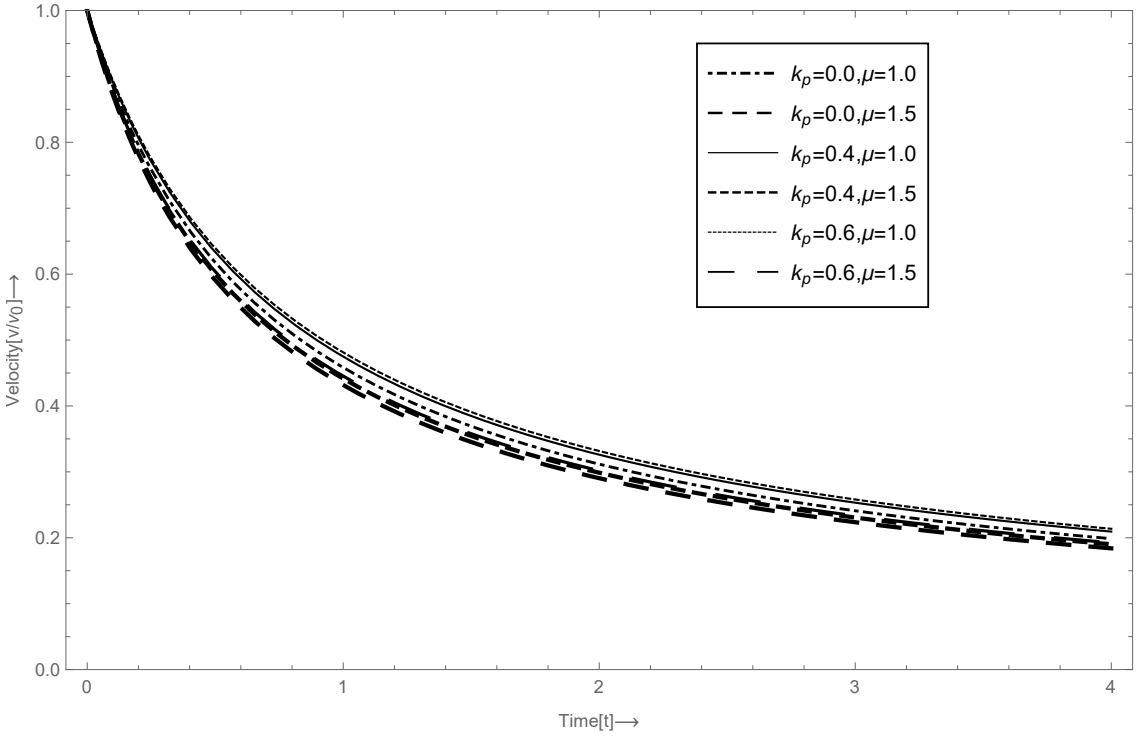

FIGURE 6.13: Variation of Velocity of sawtooth profile (v/v_0) for different value of k_p and μ with respect to time(t) with $\gamma = 1.67$, $Z_0 = 0.01$, and $\beta = 1.0$ for cylindrically symmetric flow.

****